Locomotor anatomy and biomechanics of the Dmanisi hominins

Pontzer, H ; Rolian, C ; Rightmire, G P ; Jashashvili, T ; Ponce de León, M S ; Lordkipanidze, D ; Zollikofer, C P E

Abstract: The Dmanisi hominins inhabited a northern temperate habitat in the southern Caucasus, approximately 1.8 million years ago. This is the oldest population of hominins known outside of Africa. Understanding the set of anatomical and behavioral traits that equipped this population to exploit their seasonal habitat successfully may shed light on the selection pressures shaping early members of the genus Homo and the ecological strategies that permitted the expansion of their range outside of the African subtropics. The abundant stone tools at the site, as well as taphonomic evidence for butchery, suggest that the Dmanisi hominins were active hunters or scavengers. In this study, we examine the locomotor mechanics of the Dmanisi hind limb to test the hypothesis that the inclusion of meat in the diet is associated with an increase in walking and running economy and endurance. Using comparative data from modern humans, chimpanzees, and gorillas, as well as other fossil hominins, we show that the Dmanisi hind limb was functionally similar to modern humans, with a longitudinal plantar arch, increased limb length, and human-like ankle morphology. Other aspects of the foot, specifically metatarsal morphology and tibial torsion, are less derived and similar to earlier hominins. These results are consistent with hypotheses linking hunting and scavenging to improved walking and running performance in early Homo. Primitive retentions in the Dmanisi foot suggest that locomotor evolution continued through the early Pleistocene.

DOI: https://doi.org/10.1016/j.jhevol.2010.03.006

AUTHOR QUERY FORM

ELSEVIER	**Journal:** YJHEV **Article Number:** 1441	**Please e-mail or fax your responses and any corrections to:** **E-mail:** corrections.essd@elsevier.tnq.co.in **Fax: +31 2048 52789**

Dear Author,

Any queries or remarks that have arisen during the processing of your manuscript are listed below and highlighted by flags in the proof. Please check your proof carefully and mark all corrections at the appropriate place in the proof (e.g., by using on-screen annotation in the PDF file) or compile them in a separate list.

For correction or revision of any artwork, please consult http://www.elsevier.com/artworkinstructions.

Articles in Special Issues: Please ensure that the words 'this issue' are added (in the list and text) to any references to other articles in this Special Issue.

Uncited references: References that occur in the reference list but not in the text – please position each reference in the text or delete it from the list.
Missing references: References listed below were noted in the text but are missing from the reference list – please make the list complete or remove the references from the text.

Location in article	Query / remark Please insert your reply or correction at the corresponding line in the proof
Q1	Kindly check the affiliations.
Q2	Please check the hierarchy of section headings.
Q3	The following references have been changed to match the reference list: "Hermann et al., 1998" to "Hermann and Egund, 1998""Geissman (1986)" to "Geissmann (1986)""Harcourt-Smith and Aeillo, 2004" to "Harcourt-Smith and Aiello, 2004". Please verify.
Q4	Please check the placement of footnotes citations 1–4 have been made at the end of the sentence "Parsing the independent effects…" Please check.
Q5	Kindly check the layout of the tables.
Q6	Kindly provide the significance of italics in Table 3.
Q7	Please note that there is a mention of part figures in the caption but there is no corresponding labels provided in the figure. Please verify.

Electronic file usage
Sometimes we are unable to process the electronic file of your article and/or artwork. If this is the case, we have proceeded by:

☐ Scanning (parts of) your article ☐ Rekeying (parts of) your article ☐ Scanning the artwork

Thank you for your assistance.

Journal of Human Evolution xxx (2010) 1–13

Contents lists available at ScienceDirect

Journal of Human Evolution

journal homepage: www.elsevier.com/locate/jhevol

Locomotor anatomy and biomechanics of the Dmanisi hominins

Herman Pontzer [a,*], Campbell Rolian [b], G. Philip Rightmire [c], Tea Jashashvili [d,e], Christoph P.E. Zollikofer [e], Marcia Ponce de Leon [e], David Lordkipanidze [d]

[a] Department of Anthropology, Washington University, St Louis, MO 63130, USA
[b] Department of Cell Biology & Anatomy, University of Calgary, Calgary, T2N 4N1 Alberta, Canada
[c] Department of Anthropology, Harvard University, Cambridge, MA 02138, USA
[d] Georgian National Museum, 0105 Tbilisi, Georgia
[e] Anthropologisches Institut, Universität Zürich, 8057 Zürich, Switzerland

ARTICLE INFO

Article history:
Received 18 September 2009
Accepted 2 March 2010

Keywords:
Dmanisi
Biomechanics
Early *Homo*
Hominin evolution

ABSTRACT

The Dmanisi hominins inhabited a northern temperate habitat in the southern Caucasus, approximately 1.8 million years ago. This is the oldest population of hominins known outside of Africa. Understanding the set of anatomical and behavioral traits that equipped this population to exploit their seasonal habitat successfully may shed light on the selection pressures shaping early members of the genus *Homo* and the ecological strategies that permitted the expansion of their range outside of the African subtropics. The abundant stone tools at the site, as well as taphonomic evidence for butchery, suggest that the Dmanisi hominins were active hunters or scavengers. In this study, we examine the locomotor mechanics of the Dmanisi hind limb to test the hypothesis that the inclusion of meat in the diet is associated with an increase in walking and running economy and endurance. Using comparative data from modern humans, chimpanzees, and gorillas, as well as other fossil hominins, we show that the Dmanisi hind limb was functionally similar to modern humans, with a longitudinal plantar arch, increased limb length, and human-like ankle morphology. Other aspects of the foot, specifically metatarsal morphology and tibial torsion, are less derived and similar to earlier hominins. These results are consistent with hypotheses linking hunting and scavenging to improved walking and running performance in early *Homo*. Primitive retentions in the Dmanisi foot suggest that locomotor evolution continued through the early Pleistocene.

Introduction

The locomotor anatomy of fossil hominins is notable for its variability (Aiello and Dean, 1990; Klein, 1999; Harcourt-Smith and Aiello, 2004; Conroy, 2005). Nonetheless, two broad grades of locomotor anatomy can be distinguished within the last 4 million years of hominin evolution (Klein, 1999; Bramble and Lieberman, 2004; Conroy, 2005). Members of the older group, the australopithecines, were habitual terrestrial bipeds that retained several primitive features related to arboreal locomotion, including relatively long arms and short hind limbs, long, curved phalanges, and a funnel-shaped torso with narrow shoulders and superiorly oriented glenoid fossa (Aiello and Dean, 1990; Ward, 2002; Bramble and Lieberman, 2004; Alemseged et al., 2006). In contrast, members of the genus *Homo* possess a suite of derived post-cranial traits associated with greater cursoriality, including longer hind limbs, shorter pedal phalanges, and a rigid longitudinal plantar arch (Shipman and Walker, 1989; Aiello and Dean, 1990; Bramble and Lieberman, 2004). Recently, we reported new post-cranial fossils for hominins from the site of Dmanisi that possess a mix of primitive and derived features (Lordkipanidze et al., 2007). In this paper, we assess the locomotor mechanics and energetics of these hominins and discuss the selection pressures shaping the transition from *Australopithecus* to *Homo*.

Many of the derived hind limb features of the genus *Homo* suggest improved walking and running performance relative to the australopithecines. Increased hind limb length, evident in *Homo erectus* and later hominins, decreases the energy cost of walking and running in humans (Minetti et al., 1994; Steudel-Numbers and Tilkens, 2004; Steudel-Numbers, 2006) and other terrestrial animals (Kram and Taylor, 1990; Pontzer, 2005, 2007a,b; Pontzer et al., 2009). The stiff longitudinal plantar arch, which may be present as early as *Homo habilis* (Harcourt-Smith and Aiello, 2004), improves efficiency in two ways: first, by acting as a spring during running, storing energy during midstance and returning it during toe-off (Ker et al., 1987; Alexander, 1991), and secondly, improving

* Corresponding author.
E-mail address: hpontzer@wustl.edu (H. Pontzer).

0047-2484/$ – see front matter © 2010 Published by Elsevier Ltd.
doi:10.1016/j.jhevol.2010.03.006

walking economy by providing rigidity to the foot during toe-off. The shorter toes of *Homo* decrease the digital flexor muscle work required during the second half of the stance phase (Rolian et al., 2009) and should, in principle, decrease the energy needed to swing the leg by decreasing the mass of the foot (Myers and Steudel, 1985; Browning et al., 2007). Other features, such as the fully adducted and more robust first ray, larger articular surfaces in the hind limb, derived anatomy of the gluteus maximus muscle, and enlarged calcaneal tuberosity evident in *Homo* may also improve walking and running endurance and economy (Bramble and Lieberman, 2004; Lieberman et al., 2006).

The emergence of these locomotor adaptations in the early Pleistocene has led several authors to suggest that the transition from *Australopithecus* to *Homo* reflects a change in foraging behavior and an increase in daily travel distance (Shipman and Walker, 1989; Isbell et al., 1998; Bramble and Lieberman, 2004; Pontzer, 2006). Specifically, it has been proposed that the evolution of *Homo* in the early Pleistocene marks the advent of carnivory and the inclusion of meat as a substantial proportion of the diet (Shipman and Walker, 1989; Bramble and Lieberman, 2004; Pontzer, 2006). This hypothesis is supported by the advent of stone tools and the evidence of butchery at some early Pleistocene sites (Klein, 1999). Comparative studies in extant mammals suggest that carnivory entails increased locomotor demands. Living, hunting and scavenging carnivores travel four times farther per day, on average, than similarly sized herbivores (Garland, 1983; Carbone et al., 2005). Thus, a shift in the diet to include more meat would likely necessitate increased travel and may have led to selection for endurance and economy.

Others have proposed that alternative selection pressures underlie the anatomical changes evident in the early Pleistocene. For example, the long limbs and slender build of early African *H. erectus* may be an adaptation for maintaining high activity levels in warmer climates, increasing the ratio of skin surface area to body mass to promote convective heat loss and reduce heat stress, following Allen's rule (Ruff and Walker, 1993; Walker, 1993). Alternatively, the derived body proportions of early Pleistocene *Homo* may be a pleiotropic effect of increased body size (Lovejoy, 1999), which may have increased in response to socio-ecological pressures (O'Connell et al., 1999; Wrangham et al., 1999), or to reduce mortality during childbirth associated with increased brain size (Lovejoy, 1999). Unfortunately, because warm climate, carnivory, and large body size occur together in East African sites from which early *Homo* is known, parsing the relative effects of these selection pressures has not been possible in the African fossil record.

Recent finds from the Georgian site of Dmanisi, dated to the earliest Pleistocene at 1.77 million years ago (Lordkipanidze et al., 2007), provide an important new perspective on this debate and the origin of our genus. The site of Dmanisi is located in a northern temperate climate (41° North latitude) in a region that currently maintains a climate that is approximately 17 °C cooler than the Turkana basin of Kenya (see Supplementary Information), where many early Pliocene specimens of African *H. erectus* have been recovered. The fossil hominins at Dmanisi retain a number of primitive features, including a relatively small brain (Vekua et al., 2002; Rightmire et al., 2006) and small stature (Lordkipanidze et al., 2007), compared with penecontemporary African *H. erectus*. This suggests the Dmanisi hominins were not under heat stress and did not have the larger body and brain size associated with African *H. ergaster* or *H. erectus sensu lato*. However, the numerous manuports and stone tools found at Dmanisi, as well as evidence for butchery in the form of cut marks on bovid long bones (Lordkipanidze et al., 2007), indicate some degree of carnivory in these hominins. Thus, the Dmanisi hominins provide an opportunity to test the hypothesis that the locomotor adaptations evident in early *Homo* are related to foraging demands, rather than climate or size-related pressures.

In this paper, we examine anatomical features of the Dmanisi hind limb and investigate the functional implications for locomotor performance in these hominins. Using comparative data from African apes, humans, and other fossil hominins, we test the hypothesis that the Dmanisi hominins show improved locomotor endurance and economy relative to earlier hominins. We also compare the Dmanisi hominins with African *H. erectus* and later hominins to examine the additional effects of climate and increased body size on locomotor anatomy. Finally, because the Dmanisi hominins are the oldest members of the genus *Homo* to preserve both a complete hind limb and partial foot, we examine the implications of their morphology for hominin locomotor evolution.

Materials and methods

Materials

Post-cranial fossils from the site of Dmanisi in the Republic of Georgia were reported and described previously (Lordkipanidze et al., 2007). The hind limb elements include a femur (D4167), patella (D3418), tibia (D3901), talus (D4110), medial cuneiform (D4111), first metatarsals (D2671, D3442), third metatarsals (D2021, D3479), fourth metatarsals (D2669, D4165), and fifth metatarsal (D4058). The femur, patella, tibia, talus, and three metatarsals (D2021, D4165, D4058) appear to belong to one adult individual, while the other material may belong to three smaller individuals (Lordkipanidze et al., 2007). All visible epiphyses are fused, although material from one smaller individual (D2671, D2669) is associated with subadult humeri (Lordkipanidze et al., 2007). We focus on the femur, tibia, talus, and metatarsals in this study.

Comparative data for chimpanzees (*Pan troglodytes*), gorillas (*Gorilla gorilla*), and modern humans (*Homo sapiens*) were collected at the Cleveland Museum of Natural History (Hamann–Todd Collection), Powell-Cotton Museum, American Museum of Natural History, Peabody Museum of Archeology and Ethnology (Harvard University) and the Harvard University Museum of Comparative Zoology. Ape material is primarily from wild-shot specimens. The human material is from 20th century Americans (Hamann–Todd Collection) and 15–16th century Eastern Europeans (Mistihalj Collection, Peabody Museum). Sample sizes and composition varied among analyses, as is discussed for each comparison.

Data for other fossil hominins were taken from the literature or from casts at Washington University and Harvard University. For the early modern human (EMH) and Neanderthal samples, body masses were taken from Ruff et al. (1997) while femur and tibia lengths were taken from Trinkaus (1981). The Neanderthal sample consists of nine individuals (Amud 1, La Chappelle 1, La Ferrassie 2 and 4, Spy 2, Shanidar 1, 5 and 6, and Tabun C1), while the EMH sample consists of 12 (Grotto des Enfants 4 and 5, Predmosti 3, 4, 9, 10 and 14, Skhul 4, 5 and 6, Caviglione 1, Baousso da Torre 1). For the KNM-WT 15,000 skeleton, a body mass of 51 kg was used, following a recent study of body mass estimation in juvenile humans (Ruff, 2007).

Measurements

In assessing locomotor performance in the Dmanisi hominins, we focused primarily on skeletal traits that have been directly linked to economy and efficiency in experimental studies. Specifically, we examined hind limb length, which has been shown to be the single largest anatomical determinant of locomotor cost in terrestrial animals (Pontzer, 2007a,b), and the presence of a plantar

Please cite this article in press as: Pontzer, H., et al., Locomotor anatomy and biomechanics of the Dmanisi hominins, J Hum Evol (2010), doi:10.1016/j.jhevol.2010.03.006

arch, which has been shown to improve the efficiency of the human foot (Ker et al., 1987). Hind limb length was measured in relation to estimated body mass and the presence of a plantar arch was assessed using the pattern of metatarsal torsion, as discussed below. In addition, we examined metatarsal robusticity and tibial torsion to determine whether the habitual pattern of metatarsal loading in the Dmanisi hominins was similar to that of modern humans, and whether any differences in metatarsal loading regime might be due to differences in tibial torsion. Element dimensions and torsion angles were measured as follows.

Linear dimensions

Bicondylar length of the femur (M2; Martin, 1957) and maximum length of the tibia (M1a; Martin, 1957) were measured using a custom-made osteometric board. For the Dmanisi sample, linear measurements of the tarsals and metatarsals were taken using standard digital calipers. In the extant sample, metatarsal linear measurements were collected from digital scans taken on a flatbed scanner at a resolution of 300 dpi (MicroTek i320 ScanMaker, Carson, CA, see Rolian et al., 2009 for details). The scanner method has been validated in several morphometric studies (e.g., Hallgrimsson et al., 2002; Young and Hallgrimsson, 2005), and provides several advantages over camera or caliper based methods, including reduced measurement error and parallax. Measurements for comparative fossil material were taken from the literature, or, when necessary, from casts.

Metatarsal torsion

Metatarsal torsion, measured about the long axis of each metatarsal, was calculated by comparing the major axis of the proximal and distal articular surfaces (Fig. 1C and D). The major axis was defined as the longest diameter of the articular surface. The metatarsal was rested with its proximal end on graph paper on a hard surface with the long axis of the bone standing vertically. The major axis of the proximal articular surface was aligned to coincide with a line of reference (i.e., a line on the graph paper). Sighting down, along the long axis of the bone, the projected endpoints of the major functional axis of the distal articular surface were then marked on the graph paper. These two marks were then connected with a line, and the angle included between this line (the major axis of the metatarsal head) and the reference line (the major axis of the proximal articular surface) was taken as the degree of metatarsal torsion. The graph paper was scanned and the angle was measured using ImageJ®. This method was modified for the metatarsals I and V. For metatarsal I, the sesamoid eminences on the plantar margin of the head were found to be more reliable indicators of the functional axis of the distal articular surface. The projections of these eminences were marked and used to calculate torsion angle by subtracting 90° from the angle included by the projected axis and the line of reference. For metatarsal V, the proximal articulation is oblique to the major axis of bone, and thus determining torsion was found to be easier with the metatarsal head resting on the table. With the metatarsal placed head-down and the major axis of the head coincident with the reference line, the projected major axis of the proximal articular surface was marked and the angle between the proximal and distal axes was determined as above. In order to maintain consistency among rays, 90° was subtracted to give the torsion angle because the major axis of the proximal articular surface in metatarsal V is orthogonal to those of the other metatarsals. Where distal ends are missing (i.e., in some fossil specimens) but the orientation of the shaft is clear, torsion was measured using the major axis of the distal surface of the broken shaft (Fig. 1D).

Our method for determining torsion is similar to the approach used by Largey et al. (2007), although their process for determining the articular axes differed from that used here. Largey et al. (2007) determined the proximal and distal axes based on the cross-sectional properties of the metatarsal shaft, whereas here these axes were determined as the major axes of the articular surfaces. In keeping with previous studies (Largey et al., 2007), medial rotation of the metatarsal heads (i.e., pronation) was considered positive torsion, while lateral rotation (i.e., supination) was considered negative torsion. A small intraobserver repeatability study was done to assess the reliability of our method. Ten metatarsals (two of each ray) were each measured five times using the method described above. The mean standard error of measurement for each set of five repeated measurements was ±1.3°, and the mean range of measurements for a five-measurement set was 6.9° (maximum range 12.0°). For comparison, between-group differences in metatarsal torsion for rays II–IV were typically in excess of 20° (see below).

Tibia torsion

Torsion about the long axis of the bone (i.e., torsion in the transverse plane) was measured using digital photographs (Canon®). The tibia was set on a table, posterior surface down, with its distal end near the table's edge. A photograph of the talar articular surface was then taken, with the camera oriented in the same plane as the articular surface. This process was repeated for the proximal articular surface, with the tibia's proximal end near the table edge. These digital images were then examined in ImageJ®. For the image of the distal articular surface, the midpoints of the lateral and medial margins of the articular surface were located and a line was drawn connecting these two midpoints. The angle between this

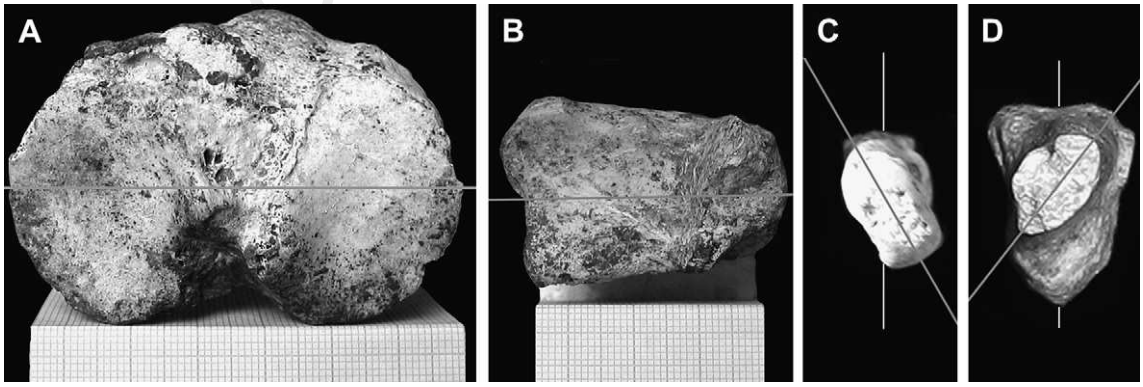

Figure 1. Measuring torsion in the tibia (A and B) and in the metatarsals (C and D). For the tibia, the angle of the proximal or talar end (gray lines) is measured with reference to the edge of the table. Note that the distal tibia is elevated slightly on a foam mat in B to protect the distal end. This was not done for all specimens. For the metatarsals, the major axis lines for the proximal and distal articular ends are shown. Metatarsals shown are left MTIV D2669 (C) and right MTIII D2021 (D).

Please cite this article in press as: Pontzer, H., et al., Locomotor anatomy and biomechanics of the Dmanisi hominins, J Hum Evol (2010), doi:10.1016/j.jhevol.2010.03.006

line and the edge of the table was used to determine the Distal Articular Angle. For the image of the proximal surface, the midpoint of the anterior–posterior axis of each condylar surface was located using ImageJ®, and a line was drawn connecting these two midpoints. The angle between this line and the edge of the table was used to determine the Proximal Articular Angle. The difference between the Proximal and Distal Articular Angles was then calculated, giving the Tibial Torsion Angle. Lateral torsion (i.e., toeing "out") was defined as positive and medial torsion (i.e., toeing "in") was defined as negative, following previous research (Martin, 1957; Hicks et al., 2007). This method is shown for the Dmanisi tibia (D3901) in Fig. 1A and B.

Analyses

Proportions and relative hind limb length

We compared linear dimensions among species to examine the size and proportion of the Dmanisi hind limb elements. Additionally, summed lengths of the femur and tibia were used to provide a measure of total hind limb length for all specimens. This approach ignores the additional hind limb length provided by the tarsals, but has the advantage of being applicable for specimens without a complete foot. We calculated a body size corrected Relative Hind Limb (RHL) length, using the formula RHL = (Femur + Tibia)/Body Mass$^{0.33}$. Calculating RHL this way assumes that limb length scales isometrically with body mass. This assumption is supported in our human sample [(Femur + Tibia) = 209.7(Estimated Mass)$^{0.331}$, $r^2 = 0.40$, $n = 86$], although we note that limb length scales with negative allometry in our gorilla sample [(Femur + Tibia) = 200.7 (Estimated Mass)$^{0.250}$, $r^2 = 0.83$, $n = 22$] and chimpanzee sample [(Femur + Tibia) = 303.3(Estimated Mass)$^{0.157}$, $r^2 = 0.30$, $n = 60$].

Body mass estimates for fossils were taken from the literature (Table 1). Body mass estimates for modern humans and apes were calculated using the intra *Homo* and Hominoid LSR regressions, respectively, for femoral head diameter, given in McHenry (1992). While this introduces some circularity since femoral dimensions are used for both hind limb length and body mass, given the importance of hind limb length in determining locomotor cost (Pontzer, 2005, 2007a,b), RHL was nonetheless viewed as useful for comparing hind limb length among species. It should be noted that other proxies of body mass generally give similar estimates of size, both in the Dmanisi sample (Lordkipanidze et al., 2007) and in extant hominoids (McHenry, 1992). Linear measurements and RHL for species and specimens included in our analyses are given in Table 1.

Plantar arch

To assess whether the Dmanisi hominin foot possessed a longitudinal plantar arch, we examined metatarsal torsion. In modern humans, the plantar arch produces a transverse arch at the midfoot, with the base of the first metatarsal held above the ground plane and the base of the fifth metatarsal resting on the ground plane. The major axes of the proximal articular surfaces are thus radially arrayed in the coronal plane; metatarsal torsion changes this arrangement so that the main axes of the distal articular surfaces are parallel to one another and oriented in the sagittal plane, with the axis of rotation for the metatarsal-phalangeal joints oriented horizontally (Fig. 2A). As noted nearly a century ago by Morton (1922), the pattern of torsion differs in apes, reflecting the lack of a transverse arch and the functional requirement of placing the first metatarsal in opposition to the other rays (Fig. 2B) (see also Lewis, 1980). We examined the pattern of metatarsal torsion in the Dmanisi hominins and compared it with the torsion patterns seen in apes and humans, as well as in the OH-8 foot. Note that other means of assessing the presence of a longitudinal plantar arch, such as cuboid or navicular morphology, could not be employed in the Dmanisi sample.

Metatarsal robusticity

First metatarsals in modern humans are substantially more robust than those of the other rays, which may reflect the mechanical stress experienced by the MTI during the second half of the stance phase and toe-off (Griffin and Richmond, 2005). To determine whether metatarsal robusticity is similar to that of modern humans, we compared metatarsal robusticity in the Dmanisi hominins with living humans and apes, and to available hominin fossils. Metatarsal robusticity was calculated as (Dorsoplantar Midshaft Diameter^2)/(Maximum Length × Body Mass). This estimate of robusticity was chosen because, following standard beam theory, the bending stress on the metatarsal shaft should increase linearly with metatarsal length and load (i.e., body mass), while the resistance to bending should increase with the square of shaft diameter. Body masses were estimated from femoral head diameter (see above) or, for fossil specimens, taken from published estimates of body size. For the Dmanisi sample, metatarsals robusticity was calculated using the body mass of the individual

Table 1
Long bone lengths and relative hind limb length (RHL) for fossil hominins, modern humans, chimpanzees, and gorillas. Q5

Taxon	*N*	Mass (kg)	Humerus (mm)		Femur (mm)		Tibia (mm)		RHL	
A.L. 288[a]		27.9	237		281		241		174	
KNM-WT 15,000[b]		51.0	319		429		380		221	
KNM-ER 1472[c]		49.6	–		401		*340*		204	
KNM-ER 1481[c]		57.0	–		396		*333*		215	
OH-34[c]		51.0	–		432		*367*		218	
OH-35[d]			–		–		*259*		–	
Dmanisi		48.8	*295*		382		306		191	
Neanderthals	9	72.8 (9.2)	–		433 (30)		342 (29)		189 (12)	
Early modern humans	12	68.0 (7.9)	–		471 (40)		401 (30)		217 (12)	
Human	F: 33	53.6 (5.2)	317	303 (19)	445	428 (27)	372	356 (28)	211	211 (13)
	M: 53	67.9 (6.2)		331 (19)		463 (28)		387 (29)		211 (12)
Chimpanzee	F: 40	39.4 (6.1)	301	299 (13)	295	292 (14)	251	247 (13)	159	161 (8)
	M: 20	46.1 (7.5)		303 (14)		299 (13)		254 (11)		157 (7)
Gorilla	F: 13	72.9 (12.3)	407	375 (19)	348	316 (14)	287	265 (11)	140	142 (5)
	M: 9	134.5 (22.3)		439 (15)		380 (12)		310 (18)		137 (7)

Lengths are in millimeters with measurement code from Martin (1957) indicated; estimated masses are in kilograms. RHL is calculated as (femur + tibia)/(estimated mass$^{0.33}$); see text. Dmanisi values are for the large adult individual (Lordkipanidze et al., 2007). Lengths in italics are estimates. Means (standard deviations) are shown for fossil and extant groups.

[a] Length estimates from Geissmann (1986), mass estimate from McHenry (1992).
[b] Length estimates from Ruff and Walker (1993); mass estimate from Ruff (2007).
[c] Length and mass estimates from Steudel-Numbers and Tilkens (2004).
[d] Length estimate from Susman and Stern (1982).

Please cite this article in press as: Pontzer, H., et al., Locomotor anatomy and biomechanics of the Dmanisi hominins, J Hum Evol (2010), doi:10.1016/j.jhevol.2010.03.006

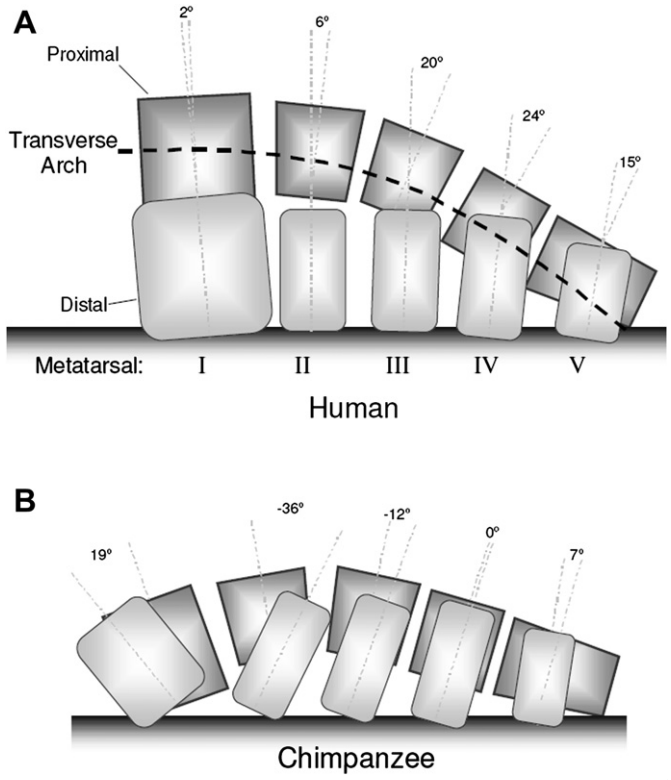

Figure 2. A. Schematic diagram of the metatarsals in the average human foot in anterior view (left foot shown). Torsion of the metatarsals (mean values shown) results from the radial arrangement of the proximal ends in the transverse arch and the parallel arrangement of the distal ends at contact with the ground plane. B. A similar diagram for the average chimpanzee foot. The proximal end of the metatarsal row contacts the substrate on the medial and lateral sides, and the distal first ray is in opposition to the lateral rays.

with which they are associated (Table 3; see Lordkipanidze et al., 2007). We used anterior–posterior (i.e., dorsal-plantar) midshaft width in order to estimate bending strength in the sagittal plane, since bending stress in the metatarsal during walking and running is expected to be greatest in the sagittal plane. One of the Dmanisi third metatarsals, D2021, is nearly complete, but is broken at the base of the metatarsal head. To provide an estimate of robusticity for this specimen, we estimated its length using the length of metatarsal IV, D2669, and the LSR equation relating metatarsal III and IV lengths in our pooled sample of humans and apes (MTIII = 0.8835 MTIV + 9.13; $r^2 = 0.91$, $n = 168$, $p < 0.001$); the estimated length (61 mm) is consistent with the morphology and length of the specimen. Another specimen, D4058, a fifth metatarsal, is also broken at the base of the head. The total length for this specimen was estimated at 62 mm, based on the preserved morphology of the head base.

In our initial description, we suggested that the Dmanisi metatarsal I was less robust, relative to the other metatarsals, than is seen in humans, and that this may be related to the lack of tibial torsion in the Dmanisi population. Greater torsion of the tibia is expected to rotate the forefoot laterally, resulting in greater stress on the medial margin of the foot during walking. In fact, plantar pressure under the first ray (metatarsal I and hallux) exceeds that of any of the other metatarsals during normal human walking and running (Hayafune et al., 1999; Nagel et al., 2008). To test the hypothesis that the increased tibial torsion seen in modern humans relative to living apes is related to differences in relative metatarsal robusticity, we plotted the degree of tibial torsion against the ratio of robusticity in metatarsals I/III or I/IV for apes, humans, and the Dmanisi hominins. We predicted a positive relationship between tibia torsion and relative robusticity of metatarsal I, since greater lateral torsion of the foot is expected to lead to greater loading of the medial rays during walking and running.

Results

Linear dimensions and morphology

Femur and patella

The Dmanisi femur (D4167) appears to be functionally similar to other Pleistocene *Homo*. The greater trochanter is less elevated than the head but is laterally prominent. There is no groove for the obturator externus tendon crossing the surface of the neck, which is compressed anteroposteriorly (Lordkipanidze et al., 2007). Anteversion (femoral torsion) is 8°, slightly below the mean for most human samples (e.g., Reikeras et al., 1983, mean = 13°, standard deviation 7°, $n = 47$), but well within the range for modern humans (−5° to +30°, see Yushiok et al., 1987; Hermann and Egund, 1998). Q3 The shaft is straight in anterior view and displays the valgus orientation (associated with a high bicondylar angle) typical of hominins. The linea aspera is situated atop a well-developed pilaster. The distal end is relatively large, with a maximum width of the condyles of 75 mm. The patellar groove is deeply concave transversely, but is vertically convex. Toward its lateral margin, the patellar surface displays an area of smoothing, and tiny perforations suggest loss of articular cartilage followed by eburnation of the bone. This pathology is reflected also by evidence from the patella (D3418), which is eburnated on the inferior portion of its lateral articular surface. This osteoarthritis does not appear to have limited knee function.

Tibia

Like the femur, the Dmanisi tibia (D3901) is robust, with large proximal and distal articular ends relative to its length (Lordkipanidze et al., 2007). The shaft is straight in the sagittal plane, with very slight bowing in the coronal plane and an oval cross-section at midshaft. The distal articulation is concave anteroposteriorly but flattened mediolaterally, and wider anteriorly (Fig. 1B). Anteriorly, the talar articulation exhibits squatting facets, with both a crescent-shaped lateral facet and a smaller medial facet present. These notches suggest contact with the talar neck during extreme dorsiflexion of the foot at the ankle, as seen in populations that regularly adopt a squatting posture (Singh, 1959). Posteriorly, the distal end exhibits a broad, channel-like groove for the tibialis posterior. Tibial torsion is very low (1°, see below).

Hind limb length and proportion

As noted in our initial description (Lordkipanidze et al., 2007), the Dmanisi hominins are of smaller stature than modern humans. This is evident in the long bone dimensions. Comparing maximum lengths of the femur and tibia, the Dmanisi hominins are absolutely larger than the A.L. 288 specimen of *Australopithecus afarensis*, the OH-35 specimen assigned to *H. habilis,* and living chimpanzees and gorillas, but substantially smaller than specimens assigned to *H. erectus,* as well as Neanderthals and modern humans (Table 1). RHL calculated from the Dmanisi femur and tibia is similarly intermediate. Body mass for this individual is estimated at 48.8 kg with a range of 46.9–50.8 kg (Lordkipanidze et al., 2007), giving an estimated RHL of 191 with a range of 188–193. These RHL values are greater than seen in living apes (gorillas: mean 140, standard deviation ±6.7; chimpanzees: 159 ± 8.0) and the A.L. 288 *A. afarensis* specimen (174), but less than the KNM-ER 1481 and KNM-ER 1472 specimens assigned to *H. habilis* (RHL of 215 and 204, respectively) or the KNM-WT 15,000 and OH-35 African *H. erectus*

Please cite this article in press as: Pontzer, H., et al., Locomotor anatomy and biomechanics of the Dmanisi hominins, J Hum Evol (2010), doi:10.1016/j.jhevol.2010.03.006

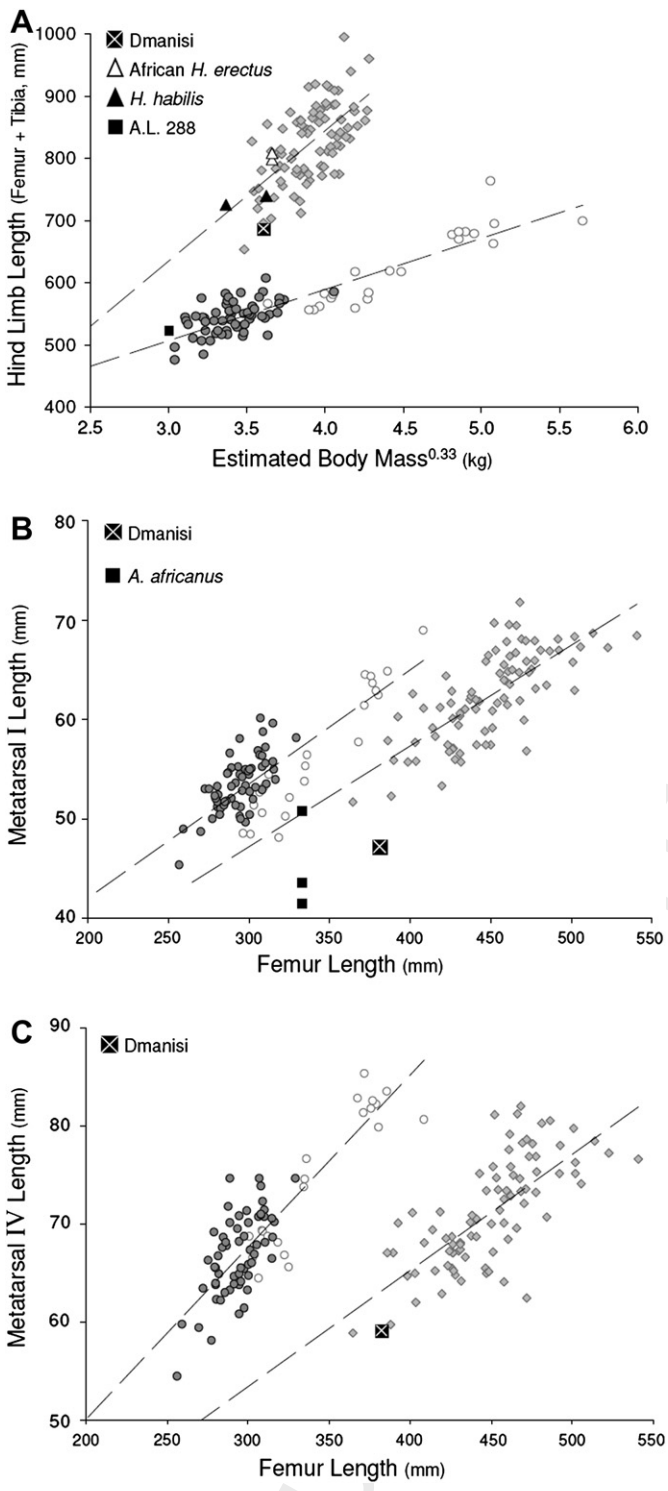

Figure 3. A. Hind limb length (femur + tibia) plotted against (estimated body mass)$^{0.33}$. Gray diamonds: modern humans; gray circles: chimpanzees; open circles: gorillas. Dashed lines are LSR equations for humans and apes (chimpanzees and gorillas combined). Black square with white ×: Dmanisi; open triangles: African *H. erectus* (KNM-WT 15,000 and OH-34); black triangles: *H. habilis* (KNM-ER 1481 and KNM-ER 1472); filled black square: A.L. 288. B. Metatarsal I length and C. metatarsal IV length versus femur length; symbols for extant groups as in A. Lengths for three metatarsal I specimens are plotted for *A. africanus* (black squares; see Table 3) against estimate femur length for this species (333 mm) from Webb (1996).

specimens (RHL of 221 and 218, respectively; Table 1). This result is consistent with previous analyses (e.g., Jungers, 1982) indicating short hind limbs in *A. afarensis* relative to modern humans. Compared with more recent *Homo*, Dmanisi RHL is most similar to our European Neanderthal sample (189 ± 12.3) and below the mean for fossil early modern humans (217 ± 12.5) and modern humans (211 ± 12.6) (Table 1; Fig. 3A). The high RHL value for the KNM-WT 15,000 specimen does not appear to be an artifact of its juvenile status and estimates of adult hind limb length and body mass for this specimen (Ruff and Walker, 1993) produce RHL values in excess of 230. As noted in our initial report, the Dmanisi hominins are like modern humans in their humero-femoral proportions. When humerus length is plotted against femur length, Dmanisi groups clearly with other members of the genus *Homo* (Fig. 3B in Lordkipanidze et al., 2007).

Crural index (100× Tibia/Femur) for the Dmanisi specimen is 80.3, which is intermediate between European Neanderthals (78.9 ± 1.7) and the means for early modern humans (85.1 ± 3.1) and modern humans (83.5 ± 3.1), and substantially below that of the KNM-WT 15,000 *H. erectus* specimen (88.6). Together, these measures suggest that the Dmanisi hominins exhibited the longer hind limbs typical of *Homo*, albeit with RHL and crural index values in the lower range of values typically observed in modern humans.

Talus

The Dmanisi talus is larger than those of living chimpanzees and fossil specimens assigned to *Australopithecus*, as well as the OH-8 *H. habilis* foot (Table 2). Instead, in terms of size and morphology, the Dmanisi talus most closely resembles that of later members of the genus *Homo*, including living humans (Fig. 4). Like modern humans, the trochlea of D4110 is strongly convex longitudinally, sellar in contour and wider anteriorly than posteriorly. It lacks the relatively deep groove evident in most chimpanzees and to a lesser extent in OH-8 (Fig. 4; see Gebo and Schwartz, 2006). Its lateral and medial borders are about equally elevated, and the articular surface does not slope toward the inside of the foot. Medially, the facet for the malleolus extends forward onto the neck but is relatively flat. There is no development of a cup-shaped depression that would receive the malleolus during dorsiflexion, as in the foot of apes (Aiello and Dean, 1990). The neck is stout and expanded transversely. It appears slightly elongated relative to that of recent *Homo*, but this elongation is not so pronounced as would be usual for an ape. The (horizontal) angle subtended by the long axis of the neck and the midline of the trochlea is similar to that in humans. The inclination angle, measuring plantar inclination of the head and neck relative to the plane of the lateral trochlea, is high and hence also human-like. Although the head itself is incomplete, its morphology suggests a symmetrical placement on the neck, and there is no indication of lateral rotation. On the superior aspect of the neck, there is a small, flat surface situated laterally, just behind the head. Although not clearly defined, this feature may be a squatting facet, complementary to depressions present on the distal tibia.

Posteriorly, the D4110 body presents two tubercles. The medial tubercle is strong and projecting, so that the passage for the tendon of flexor hallucis longus is channel-like. This channel has a slightly

Table 2
Talus dimensions, in millimeters.

Specimen	Species	Talus	
		Length	Head length
A.L. 333-75	*A. afarensis*	–	23.8
A.L. 288	*A. afarensis*	33.8	19.0
KNM-ER 1464	*H. erectus?*	45.8	26.9
KNM-ER 813	*H. erectus?*	47.3	–
KNM-ER 1476	*H. erectus?*	41.3	25.3
OH-8	*H. habilis*	36.9	23.3
Dmanisi		49.6	27.0
Human ($n = 14$)		55.4 (3.7)	32.6 (2.6)
Chimpanzee ($n = 13$)		38.3 (5.2)	21.4 (2.2)

Please cite this article in press as: Pontzer, H., et al., Locomotor anatomy and biomechanics of the Dmanisi hominins, J Hum Evol (2010), doi:10.1016/j.jhevol.2010.03.006

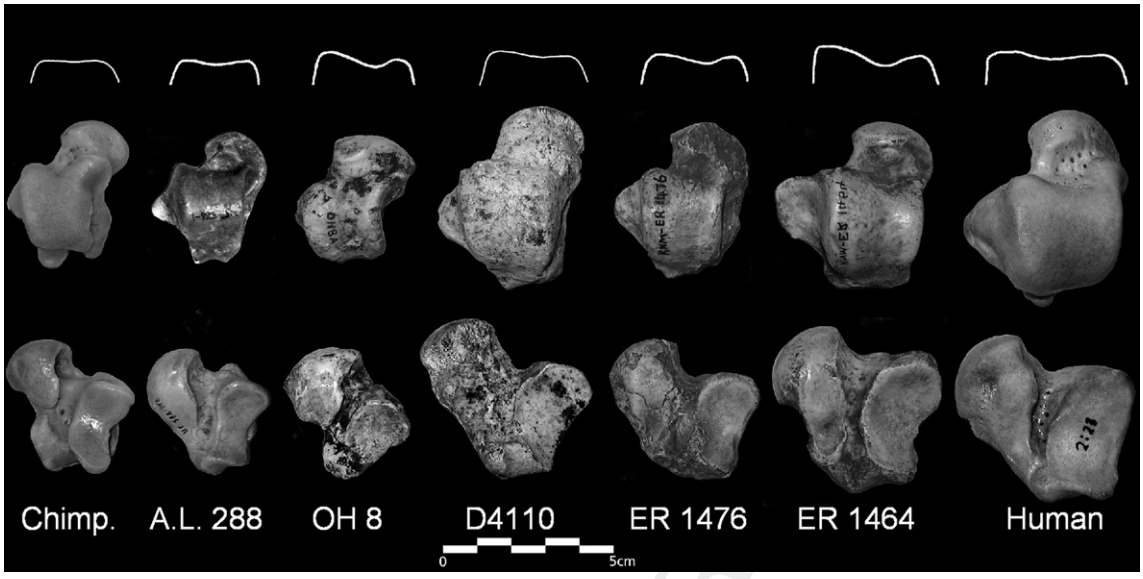

Figure 4. Trochlear profiles (white lines), and superior and inferior views of the Dmanisi talus with chimpanzee (chimp.), modern human and casts of other fossil tali. Trochlear profiles are from Gebo and Schwartz (2006), except for Dmanisi and chimpanzee. A.L. 288 and KNM-ER 1464 have been mirror-imaged.

oblique (ape-like) rather than vertical (human-like) orientation, but it is doubtful that this feature can be used to distinguish the Dmanisi talus from modern homologues. The proximal articulation for the calcaneus, while less oval than seen in most modern humans, lacks the indentation seen in chimpanzees and to a lesser extent in A.L. 288 (Fig. 4). D4110 does show some lateral projection of the talofibular articulation, a trait associated with chimpanzees rather than humans (Gebo and Schwartz, 2006), but the extent is similar to that of ER 1476, and not as extreme as ER 1464 (Fig. 4).

Metatarsals

In contrast to the talus, which is rather human-like, the Dmanisi first metatarsals are similar in size and morphology to earlier hominins, including OH-8 and specimens assigned to *Australopithecus*. The proximal shaft in both Dmanisi metatarsal I specimens is expanded, and the metatarsophalangeal articulation extends upward and curves back onto the dorsal aspect of the shaft, two features associated with human-like bipedal gait and reported previously for *A. africanus* (Susman and de Ruiter, 2004). The proximal articular surface in both D3442 and D2671 is divided into two subequal components, a feature possibly related to the bipartite medial cuneiform associated with this population (Lordkipanidze et al., 2007). Neither of these distinct facets is deeply concave, but the lower presents a raised lateral border. Notably, a similarly divided proximal articular surface is evident in the A.L. 333-54 *A. afarensis* first metatarsal. As in australopithecines and OH-8, the Dmanisi metatarsal I specimens are smaller than those of Neanderthals and modern humans (Table 2). Further, in the Dmanisi specimens, the metatarsal I heads are relatively narrow, not expanded mediolaterally as in modern humans (Fig. 5B).

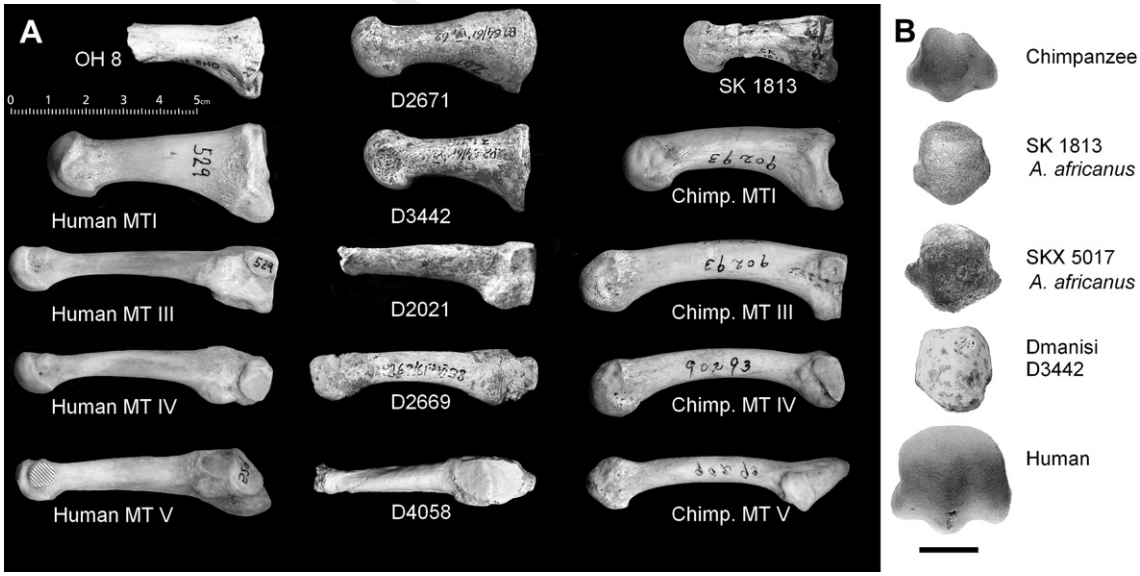

Figure 5. Comparison of metatarsal morphology. A. Profile view, Dmanisi metatarsals I, III, IV and V (middle column) compared with fossil hominins, humans, and chimpanzees. Top two rows: metatarsal I; third row, metatarsal III; fourth row, metatarsal IV; fifth row, metatarsal V. D4058 image is generated from a CT scan. Metatarsal V specimens have been mirrored to aid visual comparison with other metatarsals. Hatched area on human MTV is clay used to stabilize specimen during scanning. B. Metatarsal I heads. Scale bar: 1 cm. Adapted from Susman and de Ruiter (2004).

Please cite this article in press as: Pontzer, H., et al., Locomotor anatomy and biomechanics of the Dmanisi hominins, J Hum Evol (2010), doi:10.1016/j.jhevol.2010.03.006

The Dmanisi central and lateral metatarsals, like the metatarsal I specimens, have straight shafts in mediolateral view, and appear functionally similar to those of modern humans (Fig. 5A). However, the central and lateral metatarsals appear to be relatively longer, compared with the Dmanisi metatarsal I specimens, than is typical of modern humans. While caution must be exercised given the small sample size and estimation of lengths for some elements, the Dmanisi metatarsals III–V are 25–31% longer than the metatarsal I specimens (Table 3). This difference is similar to that seen in chimpanzees and gorillas, in which metatarsals III–V are an average of 24–28% (chimpanzees) and 31–36% (gorillas) longer than metatarsal I (Table 3). By contrast, human metatarsals III and IV average 14–15% longer than metatarsal I, and the human metatarsal V is only 4% longer, on average, than metatarsal I (Table 3). The length of the Dmanisi foot relative to that of the hind limb appears essentially modern, with ratios of metatarsal I and IV length to femur length similar to those of modern humans (Fig. 3B and C). Among hominoids, species differences in metatarsal/femur proportion derive primarily from increased femur length in hominins; the range of metatarsal lengths is similar across chimpanzees, gorillas, and humans (Fig. 3B and C).

Metatarsal robusticity

Robusticity in the first metatarsals from Dmanisi (D3442: 4.9, D2671: 5.8) fell in the upper range of values for our modern human sample (4.52 ± 0.72 $n = 86$), and well above the means for chimpanzees (3.81 ± 0.67 $n = 60$) and gorillas (2.10 ± 0.68 $n = 20$) (Fig. 6). Robust first rays appear to be common among all hominins. The robusticity values for three metatarsal I specimens assigned to *A. africanus* (4.8, 6.7, and 7.6), calculated using the estimated male body mass for this species (40.8 kg, using the intra-human formulae in McHenry, 1992) all fall above the mean for modern humans (Table 3), with the highest value exceeding the maximum robusticity value in our human sample (6.9). These robusticity values remain high even when the intra-hominoid equation is used to estimate body mass (52.8 kg), and are of course much higher if the female estimates for body mass are used.

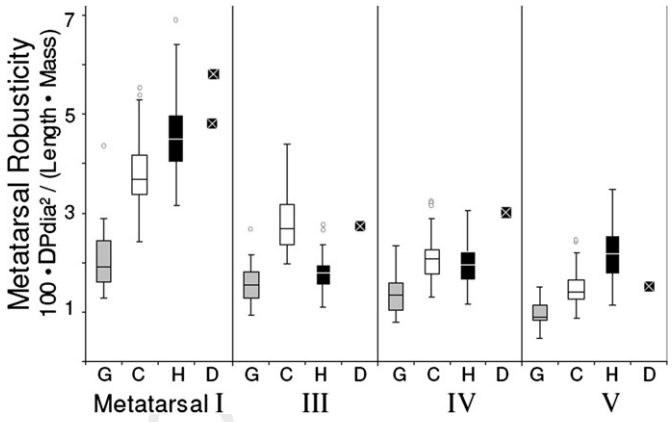

Figure 6. Boxplot showing metatarsal robusticity, calculated as (dorsoplantar midshaft diameter)^2/(length × estimated mass). Gray boxes: gorillas ($n = 20$); white boxes: chimpanzees ($n = 60$); black boxes: humans ($n = 86$); black squares with white ×: Dmanisi. Boxes indicate 25th, 50th, and 75th percentiles. Whiskers indicate sample range, excluding outliers.

Robusticity was greater for the Dmanisi metatarsal III (D2021: 2.7) and metatarsal IV (D2669: 3.0) specimens when compared with living humans. Metatarsal III robusticity in the Dmanisi sample was greater than 99% of the human specimens (1.8 ± 0.31 $n = 86$), near the mean for chimpanzees (2.8 ± 0.56 $n = 60$; Fig. 6). Metatarsal IV robusticity in Dmanisi was greater than 90% of the human specimens (2.0 ± 0.51 $n = 86$) and also exceeded the chimpanzee mean (2.1 ± 0.43 $n = 60$). In contrast, the Dmanisi metatarsal V robusticity (D4058: 1.5) fell well below the mean for modern humans (2.2 ± 0.56 $n = 86$), and closer to the mean for chimpanzees (1.5 ± 0.35 $n = 60$). The pattern of robusticity evident in the Dmanisi metatarsals, with the fifth metatarsal having the lowest robusticity, is very unusual in humans and is more common in apes (Table 3; see also Archibald et al., 1972). Further, while caution must be exercised in interpreting robusticity in the Dmanisi metatarsals given the estimation of lengths and body masses, it should be noted that the pattern of robusticity does not change when mass and length estimates are varied ±10%.

Table 3
Metatarsal dimensions. Means (standard deviations) shown for extant groups.

Species	Specimen	Length	Shaft AP Dia.	Robusticity
Metatarsal I				
A. africanus[b]	SK 1813	41.4	10.6	6.7
A. africanus[b]	SKX 5017	43.5	11.6	7.6
A. africanus[b]	Stw 562	50.7	10.0	4.8
Neanderthal[a]	Shanidar 4	60.6	12.9	3.9
Neanderthal[a]	La Ferrassie 1	60.5	11.7	2.7
Dmanisi	D2671	47.2	10.6	5.8[c]
	D3442	47.0	9.6	4.9[d]
Human ($n = 86$)		62.3 (4.5)	13.2 (1.3)	4.5 (0.7)
Chimpanzee ($n = 60$)		53.4 (2.8)	9.1 (0.9)	3.8 (0.7)
Gorilla ($n = 22$)		56.6 (6.4)	10.3 (1.2)	2.1 (0.7)
Metatarsal III				
Dmanisi	D3479	–	6.7	–
	D2021	*61*	9.0	2.7[e]
Human ($n = 86$)		72.0 (5.3)	8.9 (0.9)	1.8 (0.3)
Chimpanzee ($n = 60$)		68.2 (4.1)	8.8 (0.6)	2.8 (0.6)
Gorilla ($n = 22$)		74.1 (7.3)	10.3 (1.3)	1.6 (0.4)
Metatarsal IV				
Dmanisi	D2669	59.1	8.6	3.0[c]
Human ($n = 86$)		71.1 (5.4)	9.3 (1.4)	2.0 (0.5)
Chimpanzee ($n = 60$)		66.8 (4.2)	7.5(0.6)	2.1(0.4)
Gorilla ($n = 22$)		74.8 (7.2)	9.6(1.3)	1.4(0.4)
Metatarsal V				
Dmanisi	D4058	*62*	6.8	1.5[e]
Human ($n = 86$)		64.8 (5.0)	9.3 (1.2)	2.2 (0.6)
Chimpanzee ($n = 60$)		66.4 (4.4)	6.3 (0.6)	1.5 (0.4)
Gorilla ($n = 22$)		77.2 (9.4)	8.2 (1.4)	1.0 (0.3)

[a] Dimensions taken from casts.
[b] Dimensions taken from Susman and de Ruiter (2004).
[c] Body mass: 41.2 kg (Lordkipanidze et al., 2007).
[d] Body mass: 40.2 kg (Lordkipanidze et al., 2007).
[e] Body mass: 48.8 kg (Lordkipanidze et al., 2007).

Metatarsal robusticity and tibial torsion

Torsion in the Dmanisi tibia is very low (+1°; see Fig. 1) compared with modern humans (15.3° ± 8.9°, $n = 86$), and high compared with chimpanzees (−8.4° ± 7.9°, $n = 60$) and gorillas (−18.9° ± 6.2° $n = 22$) (Table 1). Note that this value of tibial torsion is different than the incorrect value reported initially (Lordkipanidze et al., 2007). The degree of torsion in the Dmanisi tibia is lower than all but one specimen from our modern human sample (Fig. 7). In contrast, tibial torsion in the Nariokotome specimen KNM-WT 15,000 (34°) and other Pleistocene hominins is at or above the mean for modern humans. While caution must be used in interpreting tibial torsion from reconstructed specimens, such as KNM-WT 15,000 with its hafted distal epiphysis, torsion in the Dmanisi tibia clearly falls well below that of other Pleistocene specimens. Further, it should be noted that femoral torsion in the Dmanisi hind limb does not compensate for the lack of tibial

Please cite this article in press as: Pontzer, H., et al., Locomotor anatomy and biomechanics of the Dmanisi hominins, J Hum Evol (2010), doi:10.1016/j.jhevol.2010.03.006

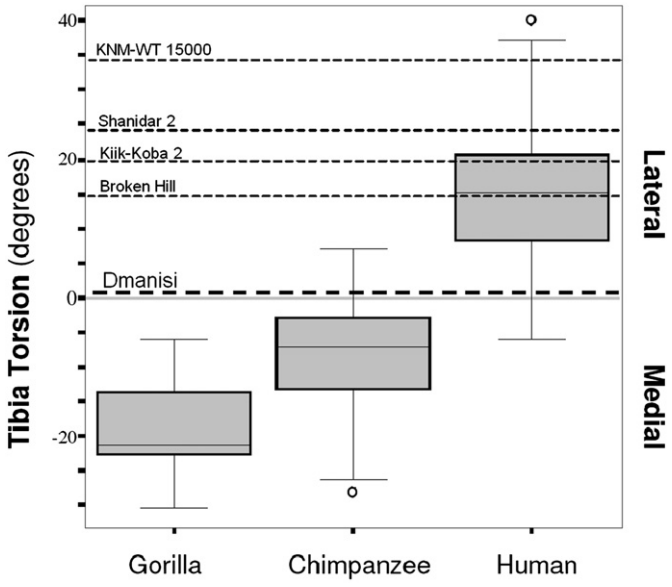

Figure 7. Tibial torsion. Lateral torsion is positive; medial is negative. Boxes indicate 25th, 50th, and 75th percentiles. Whiskers indicate sample range, excluding outliers. Data for middle Pleistocene *Homo* (Broken Hill) and Neanderthals (Kiik-Koba and Shanidar) from Wallace et al. (2008).

torsion. The combined femoral + tibial torsion in the Dmanisi hind limb results in a net −7° rotation (intoeing), well below typical net rotation in modern humans (+20°, Rittmeister et al., 2006).

Plotting tibial torsion against the relative robusticity of the first and lateral rays, it is apparent that humans exceed chimpanzees and gorillas in terms of both torsion and relative robusticity of the first metatarsal (Fig. 8). Here again, the Dmanisi hominins are intermediate between chimpanzees and humans in both tibial torsion and metatarsal robusticity. However, while there is a correlation among species between tibia torsion and relative metatarsal robusticity (MTI/III: $r^2 = 0.35$, $p < 0.01$; MTI/IV: $r^2 = 0.57$, $p < 0.01$; $n = 169$ with species pooled), there is no significant correlation within species ($p > 0.05$ all comparisons). Thus, while metatarsal robusticity does appear to correspond with tibia torsion among species, these variables do not appear to be linked within species.

Plantar arch

Metatarsal torsion in the Dmanisi hominins is similar to that seen in modern humans (Fig. 9A; Table 4). The first metatarsals of humans and chimpanzees are significantly different in terms of torsion ($p = 0.006$ Student's two-tailed t-test), but the range of variation in both species is substantial. Similarly, mean torsion in metatarsal V is statistically different between humans and chimpanzees ($p = 0.04$), but the ranges overlap considerably. However, torsion in the second, third, and fourth metatarsals are distinctly different between species ($p < 0.001$ all comparisons). While torsion of the Dmanisi first and fifth metatarsals is within the range of values seen in both chimpanzees and humans, torsion in the Dmanisi metatarsal III and IV falls within the human range, well outside of the chimpanzee range. A similar pattern of torsion is evident in the OH-8 foot (Fig. 9A). For both the Dmanisi and Olduvai specimens, a human-like pattern of metatarsal torsion is likely and this indicates the presence of a human-like transverse arch (Fig. 9B), because the absence of a transverse arch would bring the functional axes of the metatarsal-phalangeal joints out of alignment (Fig. 9C).

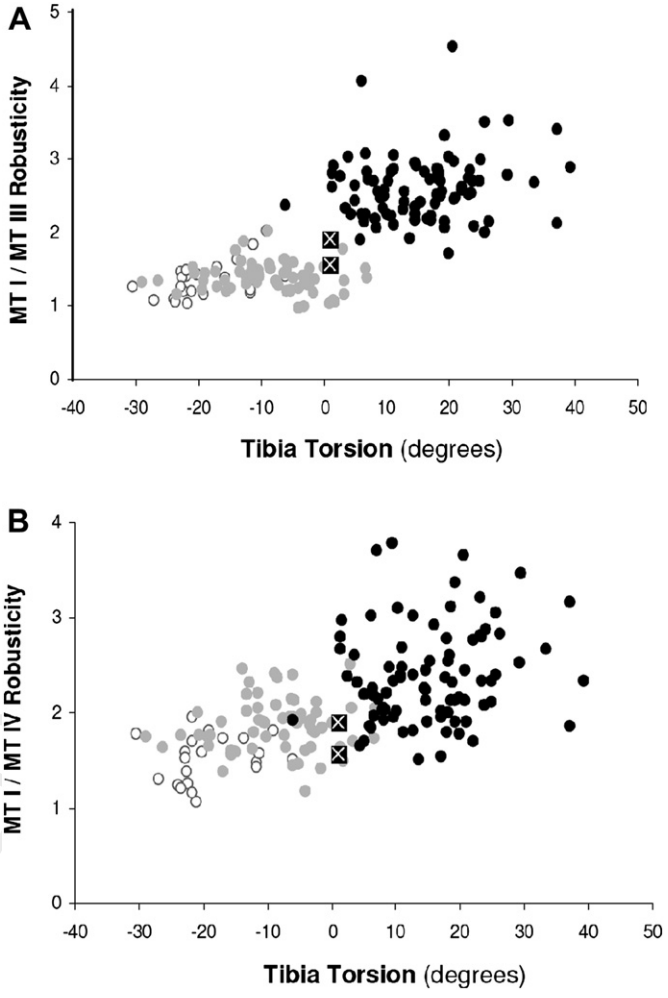

Figure 8. A. The ratio of metatarsal I robusticity to metatarsal III robusticity plotted against tibia torsion. B. The ratio of metatarsal I robusticity to metatarsal IV robusticity plotted against tibia torsion. Open circles: gorillas; gray circles: chimpanzees, black circles: humans; black square with white ×, Dmanisi. Dmanisi values are calculated using both D2671 and D3442 first metatarsals.

Discussion

Dmanisi biomechanics and the origin of Homo

Hypotheses for the emergence of the genus *Homo* often propose that the derived locomotor anatomy seen in early members of the genus reflects increased ranging due to increased meat consumption and selection for improved economy and endurance (Shipman and Walker, 1989; Bramble and Lieberman, 2004; Pontzer, 2006). The Dmanisi hominins provide an opportunity to examine the possible effects of carnivory on post-cranial anatomy without the confounding effects of heat stress and increased body and brain size present in East African populations of Pleistocene *H. erectus*. Results of this study suggest that, despite a number of primitive retentions in foot morphology, the Dmanisi hominins were more cursorially adapted than earlier hominins.

Among terrestrial species, the greatest single anatomical predictor of locomotor economy is effective limb length, the length of the hind limb as a strut (Kram and Taylor, 1990; Pontzer, 2005, 2007a,b). In fact, limb length drives the scaling of mass-specific locomotor cost (i.e., metabolic energy per kilogram body mass per distance traveled) from ants to elephants (Pontzer, 2007a), and is a better predictor of mass-specific locomotor cost than body mass.

Please cite this article in press as: Pontzer, H., et al., Locomotor anatomy and biomechanics of the Dmanisi hominins, J Hum Evol (2010), doi:10.1016/j.jhevol.2010.03.006

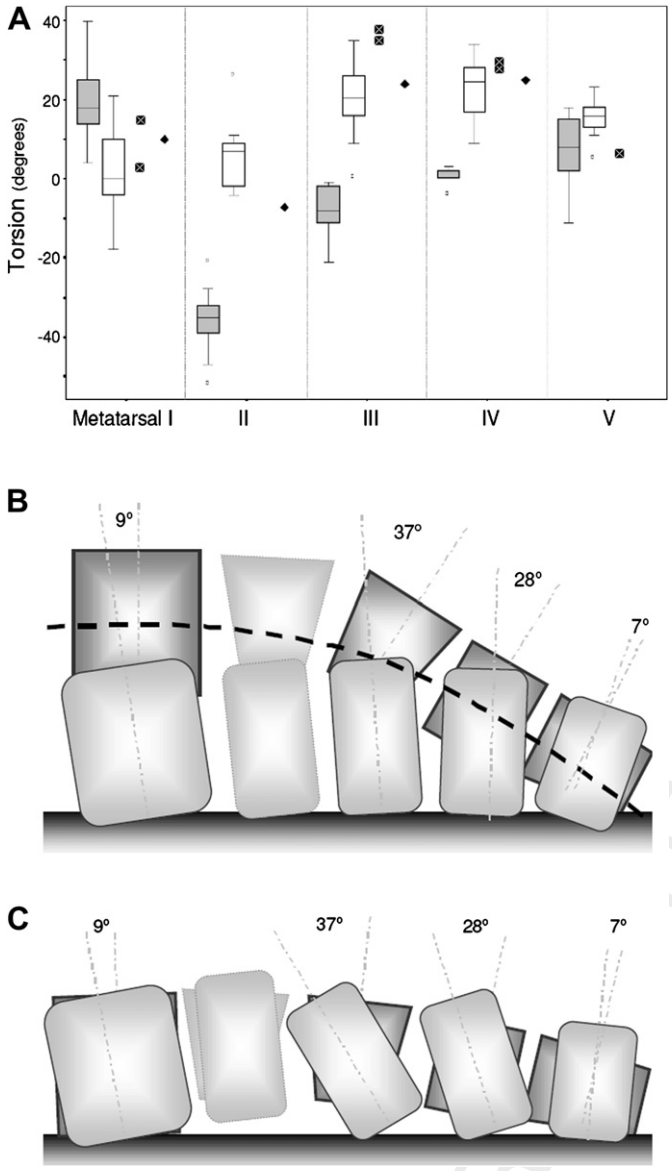

Figure 9. A. Boxplots of metatarsal torsion in chimpanzees (gray) and humans (white), compared with Dmanisi (black square with white ×) and OH-8 (black diamonds). Boxes indicate 25th, 50th, and 75th percentiles and whiskers indicate sample ranges, excluding outliers. Positive values indicate medial rotation of the distal end. B. and C. Schematic diagram of the Dmanisi foot. B. AP projection with a transverse arch. C. AP projection with no transverse arch. See also Fig. 2.

Species with particularly long limbs for their body mass have a relatively low cost of transport (i.e., energy spent per distance), while species with short limbs have high locomotor costs (Pontzer, 2007a). The effect of limb length on cost is also evident within species (Minetti et al., 1994; Steudel-Numbers and Tilkens, 2004; Pontzer, 2007b). Limb length comparisons suggest the Dmanisi hominins were intermediate between the australopithecines and later members of the genus *Homo* in terms of locomotor economy. Relative to body mass, the Dmanisi hind limb is clearly longer than that of African apes and the A.L. 288 *A. afarensis* specimen. In fact, the Dmanisi specimen is within the lower range of values for modern humans (Table 1, Fig. 3A).

While Dmanisi metatarsal morphology differs somewhat from that of later *Homo* (Fig. 5; Table 3), the Dmanisi foot appears functionally similar to that of modern humans. Among our comparative sample, the size and morphology of the Dmanisi talus is most like that of African *H. erectus* and modern humans (Table 2, Fig. 4), with a trochlea that is broad and flat (unlike OH-8). This suggests a human-like ankle joint with increased surface area for transmitting joint reaction forces associated with walking and running (DeSilva, 2009). Further, the pattern of metatarsal torsion indicates the presence of a human-like midfoot transverse arch (Fig. 9B), since the lack of a transverse arch would require that the metatarsal-phalangeal joints of the lateral rays splay laterally, a condition that is functionally implausible and unseen in humans or other apes (Fig. 9C). The presence of a midfoot transverse arch in turn indicates the presence of a longitudinal plantar arch and a concomitant improvement in locomotor efficiency (Ker et al., 1987; Alexander, 1991; Bramble and Lieberman, 2004). Without a calcaneus, cuboid, and navicular, it is impossible to know whether the arch of the Dmanisi foot was similar in some critical aspects, such as an immobile (close-packed) calcaneal-cuboid articulation, to that of later hominins (Harcourt-Smith and Aiello, 2004). However, the talar morphology, presence of an arch, and an adducted, robust first metatarsal suggest the Dmanisi foot was fully committed to terrestrial bipedalism and functionally equivalent, in terms of rigidity during stance phase and toe-off, to that of modern humans.

With a relatively long hind limb, arched foot, fully adducted and robust first ray, and human-like ankle joint, the Dmanisi hind limb appears to have been similar in most functional aspects to modern humans. Relative to the australopithecines, the Dmanisi hominins evince improved economy and efficiency in both walking and running. Since the Dmanisi hominins are associated with clear evidence of stone tool use and butchery (Lordkipanidze et al., 2007), their cursorial adaptations support the hypothesis that the adoption of meat eating in early *Homo*, either through hunting or scavenging, resulted in selection for more economical walking and running. Other proposed pressures, namely warmer temperatures (Walker, 1993) and increased body and brain size (Lovejoy, 1999) were absent for these hominins.

Locomotor evolution in the genus Homo

While our analyses focus on locomotor economy in the Dmanisi hominins, numerous and sometimes competing evolutionary pressures undoubtedly act in concert to shape locomotor anatomy. Indeed, the low crural index of the Dmanisi hind limb may be indicative of competing selection pressures. While the hind limb overall is longer than in australopithecines, the tibia is relatively short, which may be a response to the cold winter temperatures

Table 4
Metatarsal torsion. Estimates from incomplete specimens are in italics. Means (standard deviation) shown for extant groups.

Species	Torsion (degrees)				
	Specimen metatarsal I	II	III	IV	V
OH-8	*10*	*−7*	*24*	*25*	–
Dmanisi	D2671 3 D3442 15	–	D3479 *35* D2021 *38*	D2669 29	D4058 *7*
Human ($n = 10$)	2.2 (11.5)	5.6 (8.2)	20.4 (9.6)	23.6 (7.1)	15.3 (4.6)
Chimpanzee ($n = 9$)	19.1 (11.6)	−36.1 (9.3)	−7.6 (6.6)	−0.1 (2.5)	6.9 (10.1)

Please cite this article in press as: Pontzer, H., et al., Locomotor anatomy and biomechanics of the Dmanisi hominins, J Hum Evol (2010), doi:10.1016/j.jhevol.2010.03.006

(Trinkaus, 1981) typical of the southern Caucasus (see Supplementary Information). Conversely, the longer limbs and high crural index in KNM-WT 15,000 may reflect the aligned pressures of locomotor economy and thermoregulation in that population. In addition, the small, broad pelvis from Gona, Ethiopia, dated to between 0.9 and 1.4 mya (Simpson et al., 2008), underscores the importance of neonatal head size and mechanics of parturition in shaping hominin locomotor anatomy, particularly as brain size increased through the Pleistocene. Parsing the independent effects of these and other selection pressures on the hominin locomotor skeleton, as well as identifying patterns of pleiotropy and other non-adaptive change, remains an important goal for those reconstructing hominin locomotor evolution.[1–4]

The results of this study support the hypothesis that the adoption of carnivory led to selection for improved terrestrial bipedalism and the post-cranial changes seen in early Pleistocene *Homo*, but determining the precise timing and extent of evolutionary change in the hominin hind limb through the late Pliocene and early Pleistocene remains difficult. Comparisons to the australopithecines are limited to a small number of specimens of *A. afarensis* and *A. africanus* that are both temporally and geographically distant, while elements for early Pleistocene hominins are scarce and generally fragmentary. For example, the RHL estimates for KNM-ER 1481 and KNM-ER 1472, typically assigned to *H. habilis* and marginally older than the Dmanisi fossils (Klein, 1999), may suggest that increased hind limb length preceded the hominin expansion into Eurasia. However, limb proportions for *H. habilis* are uncertain (Haeusler and McHenry, 2004), making it difficult to assess whether the Dmanisi hominins are more or less derived in terms of hind limb length. Comparing the Dmanisi and OH-8 foot is useful but inconclusive. The OH-8 specimen is similar in metatarsal morphology and the presence of an arch, but seemingly more primitive in talar morphology and overall size. The combination of derived and primitive features in OH-8 and the Dmanisi foot highlights the complex nature of morphological evolution in the hominin hind limb (Harcourt-Smith and Aiello, 2004) and underscores the need for more information before competing evolutionary scenarios, either the simple carnivory model discussed here or others, can be assessed with greater confidence.

Foot mechanics of early Homo

Dmanisi is the only early Pleistocene hominin population for which a complete femur, tibia, and associated foot bones have been found, and it is therefore useful in establishing the pattern of hind limb traits evident in early *Homo*. As discussed above, the hind limb appears to be functionally similar to later members of the genus *Homo*, yet metatarsal morphology and tibial torsion are relatively primitive. The metatarsals appear to be similar in size and morphology to OH-8 and earlier hominins, and less like those of modern humans. The lengths of metatarsals III, IV and V relative to metatarsal I appear to be more similar to the condition seen in apes than in modern humans (Table 3). While the Dmanisi metatarsal I is robust and morphologically commensurate with human-like bipedalism, in lateral view the Dmanisi metatarsal I specimens are more similar to those of OH-8, as well as specimens assigned to *A. africanus* (Susman and de Ruiter, 2004), than to modern humans (Fig. 5A). Further, the phalangeal articulation of the Dmanisi first metatarsals is tall and narrow, like that of australopithecines, and lacks the mediolateral expansion seen in modern humans (Fig. 5B). The degree of torsion in the Dmanisi tibia (1°) also differs substantially from the modern human mean (15.3°). It is lower than all but 1% of the humans in our sample and lower than that of other Pleistocene hominins (Fig. 7).

The high relative robusticity of the central metatarsals III and IV, as well as the low robusticity of the Dmanisi metatarsal V (Fig. 6), suggests a loading regime in the Dmanisi that is different than in modern humans. In our initial report (Lordkipanidze et al., 2007), we suggested that the greater robusticity of the lateral metatarsals (III–V) in the Dmanisi hominins may be related to the lack of tibial torsion, since the absence of lateral tibial torsion will tend to rotate the foot medially relative to modern humans (Fig. 10), which should result in increased plantar pressures under the lateral rays during walking and running. Our data provide only weak support for this hypothesis. Tibial torsion and the relative robusticity of the central rays (III and IV) are correlated across hominoids, but are not correlated within humans, chimpanzees, or gorillas (Fig. 8). Further, humans, which have the highest degree of tibial torsion, also have the highest average metatarsal V robusticity, while the Dmanisi metatarsal V robusticity is comparatively low (Fig. 6).

At least two issues complicate the relationship between tibial torsion and metatarsal robusticity. First, as noted in a previous critique of this hypothesis (Wallace et al., 2008), other variables, such as femoral anteversion, affect the position of the foot, and it may be that tibial torsion by itself is a poor predictor of foot position and metatarsal loading. Second, the relative robusticity of metatarsals II–V does not appear to correlate strongly with the relative magnitudes of strain experienced during walking and running in humans (Griffin and Richmond, 2005). For example, plantar pressure readings during walking and running in humans (Hayafune et al., 1999; Nagel et al., 2008), as well as *in vitro* strain measures during simulated walking in cadaveric feet (Donahue and Sharkey, 1999), indicate that stresses are greater in metatarsal II than metatarsal V, but the robusticity of the fifth metatarsal significantly exceeds that of the second (Griffin and Richmond, 2005). Further, soft tissues, including the plantar fascia and digital flexors, affect the magnitude of stresses experienced by the metatarsals (Donahue and Sharkey, 1999). Thus, while we find it unlikely that tibial torsion is unrelated to foot position or that foot position is unrelated to metatarsal loading regime, a more sophisticated model of mechanical loading in the forefoot and a better understanding of non-mechanical influences on metatarsal morphology are needed to understand how tibial rotation and metatarsal robusticity reflect the locomotor mechanics and evolutionary history of the Dmanisi hominins. Future work might examine the effect of net long bone rotation (i.e., femur + tibia) and tarsal morphology on plantar pressure distribution in living humans. The effect of lateral foot rotation on locomotor performance also warrants further study. The limited work on this topic has suggested that improved sprint performance is correlated with a low positive degree of lateral foot rotation (Fuchs and Staheli, 1996).

The similarities between the OH-8 and Dmanisi feet suggest that the primitive retentions evident in both may have been common among populations of *Homo* in the early Pleistocene. The more derived foot anatomy indicated by the hominin footprints at Ileret, dated to 1.5 mya (Bennett et al., 2009) suggests that these primitive retentions were lost later, as hominin locomotor evolution continued through the Pleistocene. The primitive features of the Dmanisi and OH-8 feet might also help explain some of the features

[1] When the rigidity of the arch is effectively compromised, as during walking over loose sand (Lejeune et al., 1998), the effort to move the center of mass and the energetic cost of walking increases significantly.

[2] Here, we follow the International Commission on Stratigraphy in placing the base of the Pleistocene at 2.59 mya.

[3] Landmark-based estimates, following the Martin (1957) protocol, give a range of torsion values from −2° to +2°.

[4] Regrettably, this critique used a torsion value of 21.9° for the Dmanisi tibia, reflecting an error in our initial report (Lordkipanidze et al., 2007). As noted above, the correct value is 1° (see Table 1 and Fig. 1).

Please cite this article in press as: Pontzer, H., et al., Locomotor anatomy and biomechanics of the Dmanisi hominins, J Hum Evol (2010), doi:10.1016/j.jhevol.2010.03.006

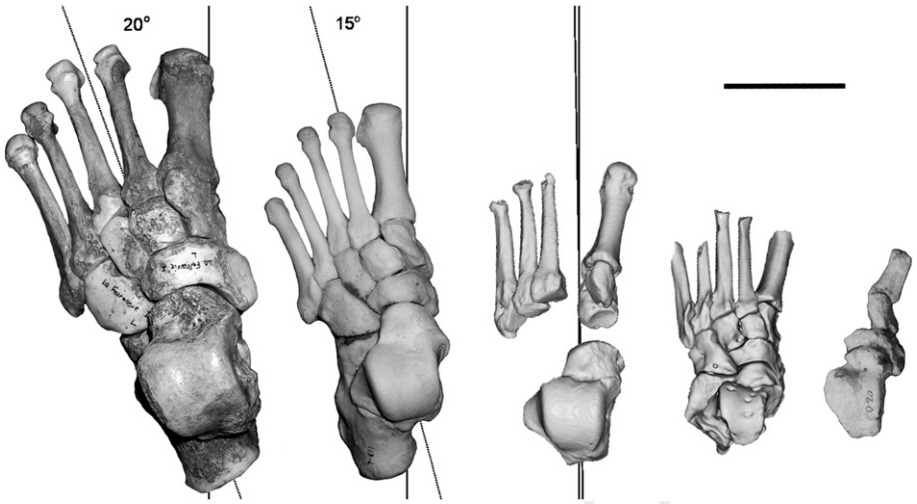

Figure 10. Superior views of the foot in A. Neanderthals (La Ferrassie 1), B. modern humans, and C. Dmanisi (composite from CT-scans), showing the effect of tibial torsion on foot position. The dashed line, indicating the lateral torsion of the tibia, is aligned here with the trochlea of the talus. Lateral rotation of the foot in Pleistocene hominins and modern humans aligns the first ray with the direction of travel (solid line), and the greatest plantar pressures are experienced by the first metatarsal during the toe-off portion of stance phase in walking and running. The absence of tibial torsion in the Dmanisi hominins is expected to result in relatively greater stresses for the lateral rays compared with humans and other Pleistocene hominins. D. OH-8 (from CT-scans of casts), and **E**. STW 573 (from Clarke and Tobias, 1995) are also shown. Scale bar: 5 cm.

seen in the *H. floresiensis* foot (Jungers et al., 2009). If the population from which *H. floresiensis* diverged was relatively primitive in its foot morphology, fewer evolutionary changes might be needed to produce the distinct set of traits seen in the Liang Bua foot.

Conclusion

Analyses of the Dmanisi skulls have demonstrated that these hominins are primitive in many respects relative to other early Pleistocene *Homo*, and similar in some cranial dimensions, including endocranial volume, to *H. habilis* (Vekua et al., 2002; Rightmire et al., 2006). We find this parallel echoed in the functional morphology of the Dmanisi hind limb with its mosaic of primitive and derived traits. The presence of an arch, human-like talus, and increased relative hind limb length in this population are suggestive of selection for improved locomotor economy and efficiency. These traits, along with the numerous stone artifacts and taphonomic traces that provide evidence for butchery at the site, are consistent with the hypothesis that early *Homo* was adapted to some degree of carnivory (hunting, scavenging, or both) and the increased locomotor demands that this foraging strategy entails (Shipman and Walker, 1989; Bramble and Lieberman, 2004; Carbone et al., 2005; Pontzer, 2006). Further, the location of Dmanisi, in an open, temperate habitat far from the African tropics, strengthens the hypothesis that this foraging strategy was critical in the expansion of early *Homo* throughout Africa and into Asia (Shipman and Walker, 1989). Intriguingly, the Dmanisi hominins are less derived in terms of hind limb length, and possibly metatarsal morphology, than African *H. erectus* specimens roughly 200,000 years younger (KNM-WT 15,000). This may suggest that selection pressure for improved walking and running performance continued through the early and middle Pleistocene. More fossils from this period, sampled from more localities, will help elucidate the undoubtedly complicated origins of our genus, and provide a more complete perspective on the early Pleistocene population at Dmanisi.

Acknowledgements

We thank David Raichlen, Daniel Lieberman, and three reviewers for comments that improved this manuscript. Cara Ocobock assisted with manuscript preparation. This work was supported by the Georgian National Science Foundation, a Rolex Award for Enterprise, BP Georgia, the Fundación Duques de Soria, and the Swiss National Science Foundation. Support was also provided by the Washington University Department of Anthropology, the Harvard University Department of Anthropology, a Harbison Faculty Fellowship to HP, a National Science Foundation Doctoral Dissertation Improvement Grant (BCS 0647624) to CR, and National Science Foundation, Leakey Foundation, and American Philosophical Society awards to GPR.

Appendix. Supplementary data

Supplementary data associated with this article can be found in the online version, at doi:10.1016/j.jhevol.2010.03.006.

References

Aiello, L., Dean, C., 1990. An Introduction to Human Evolutionary Anatomy. Academic Press, San Diego.
Alemseged, Z., Spoor, F., Kimbel, W.H., Bobe, R., Geraads, D., Reed, D., Wynn, J.G., 2006. A juvenile early hominin skeleton from Dikika, Ethiopia. Nature 443, 296–301.
Alexander, R.M., 1991. Energy saving mechanisms in walking and running. J. Exp. Biol. 160, 55–69.
Archibald, J.D., Lovejoy, C.O., Heiple, K.G., 1972. Implications of relative robusticity in the Olduvai Metatarsus. Am. J. Phys. Anthropol. 37, 93–95.
Bennett, M.R., John, W.K., Harris, J.W.K., Richmond, B.G., Braun, D.R., Mbua, E., Kiura, P., Olago, D., Kibunjia, M., Omuobo, C., Behrensmeyer, A.K., Huddart, D., Gonzalez, C., 2009. Early hominin foot morphology based on 1.5-million-year-old footprints from Ileret, Kenya. Science 323, 1197–1201.
Bramble, D.M., Lieberman, D.E., 2004. Endurance running and the evolution of *Homo*. Nature 432, 345–352.
Browning, R.C., Modica, J.R., Kram, R., Goswami, A., 2007. The effects of adding mass to the legs on the energetics and biomechanics of walking. Med. Sci. Sports Exerc. 39, 515–525.
Carbone, C., Cowlishaw, G., Isaac, N.J.B., Rowcliffe, J.M., 2005. How far do animals go? Determinants of day range in mammals. Am. Nat. 165, 290–297.
Clarke, R.J., Tobias, P.V., 1995. Sterkfontein Member 2 foot bones of the oldest South African hominid. Science 269, 521–524.
Conroy, G.C., 2005. Reconstructing Human Origins: a Modern Synthesis, second ed. Norton, New York.
DeSilva, J.M., 2009. Functional morphology of the ankle and the likelihood of climbing in early hominins. Proc. Natl. Acad. Sci. U.S.A. 106, 6567–6572.
Donahue, S.W., Sharkey, N.A., 1999. Strains in the metatarsals during the stance phase of gait: implications for stress fractures. J. Bone Joint Surg. 81, 1236–1243.
Fuchs, R., Staheli, L.T., 1996. Sprinting and intoeing. J. Pediatr. Orthop. 4, 489–491.

Please cite this article in press as: Pontzer, H., et al., Locomotor anatomy and biomechanics of the Dmanisi hominins, J Hum Evol (2010), doi:10.1016/j.jhevol.2010.03.006

Garland Jr., T., 1983. Scaling the ecological cost of transport to body mass in terrestrial mammals. Am. Nat. 121, 571–587.
Gebo, D.L., Schwartz, G.T., 2006. Foot bones from Omo: implications for hominid evolution. Am. J. Phys. Anthropol. 129, 499–511.
Geissmann, T., 1986. Estimation of australopithecine stature from long bones A.L. 288-1 as a test case. Folia Primatol. 47, 119–127.
Griffin, N.L., Richmond, B.G., 2005. Cross-sectional geometry of the human forefoot. Bone 37, 253–260.
Haeusler, M., McHenry, H.M., 2004. Body proportions of *Homo habilis* reviewed. J. Hum. Evol. 46, 433–465.
Hallgrimsson, B., Willmore, K., Hall, B., 2002. Canalization, developmental stability, and morphological integration in primate limbs. Yearbk. Phys. Anthropol. 45, 131–158.
Harcourt-Smith, W.E., Aiello, L.C., 2004. Fossils, feet and the evolution of human bipedal locomotion. J. Anat. 204, 403–416.
Hayafune, N., Hayafune, Y., Jacob, H., 1999. Pressure and force distribution characteristics under the normal foot during the push-off phase in gait. Foot 9, 88–92.
Hermann, K.L., Egund, N., 1998. Measuring anteversion in the femoral neck from routine radiographs. Acta Radiol. 39, 410–415.
Hicks, J., Arnol, A., Anderson, F., Schwartz, M., Delp, S., 2007. The effect of excessive tibial torsion on the capacity of muscles to extend the hip and knee during single-limb stance. Gait Posture 26, 546–552.
Isbell, L.A., Pruetz, J.D., Lewis, M., Young, T.P., 1998. Locomotor activity difference between sympatric Patas monkeys (*Erythrocebus patas*) and Vervet monkeys (*Cercopithecus aethiops*): implications for the evolution of long hindlimb length in *Homo*. Am. J. Phys. Anthropol. 105, 199–208.
Jungers, W.L., 1982. Lucy's limbs: skeletal allometry and locomotion in *Australopithecus afarensis*. Nature 297, 676–678.
Jungers, W.L., Harcourt-Smith, W.E.H., Wunderlich, R.E., Tocheri, M.W., Larson, S.G., Sutikna, T., Awe Due, Rhokus, Morwood, M.J., 2009. The foot of *Homo floresiensis*. Nature 459, 81–84.
Ker, R.F., Bennett, M.B., Bibby, S.R., Kester, R.C., Alexander, R.McN, 1987. The spring in the arch of the human foot. Nature 325, 147–149.
Klein, R.G., 1999. The Human Career, second ed. Chicago Univ. Press, Chicago.
Kram, R., Taylor, C.R., 1990. Energetics of running: a new perspective. Nature 346, 265–267.
Largey, A., Bonnel, F., Canovas, F., Subsol, G., Chemouny, S., Frédéric Banegas, F., 2007. Three-dimensional analysis of the intrinsic anatomy of the metatarsal bones. J. Foot Ankle Surg. 46, 434–441.
Lejeune, T.M., Willems, P.A., Heglund, N.C., 1998. Mechanics and energetics of human locomotion on sand. J. Exp. Biol. 201, 2071–2080.
Lewis, O.J., 1980. The joints of the evolving foot. Part III. The fossil evidence. J. Anat. 131, 275–298.
Lieberman, D.E., Raichlen, D.A., Pontzer, H., Bramble, D.M., Cutright-Smith, E., 2006. The human gluteus maximus muscle and its role in running. J. Exp. Biol. 209, 2143–2155.
Lordkipanidze, D., Jashashvili, T., Vekua, V., Ponce de Leon, M.S., Zollikofer, C.P.E., Rightmire, G.P., Pontzer, H., Ferring, R., Oms, O., Tappen, M., Bukhsianidze, M., Agusti, J., Kahlke, R., Kiladze, G., Martinez-Navarro, B., Mouskhelishvili, A., Nioradze, M., Rook, L., 2007. Postcranial evidence from early *Homo* from Dmanisi, Georgia. Nature 449, 305–310.
Lovejoy, C.O., 1999. The natural history of human gait and posture. Part 1. Spine and pelvis. Gait Posture 21, 95–112.
Martin, R., 1957. Lehrbuch der Anthropologie in Systematischer Darstellung mit Besonderer Berücksichtigung der Anthropologischen Methoden. Fischer, Stuttgart.
McHenry, H., 1992. Body size and proportions in early hominids. Am. J. Phys. Anthropol. 87, 407–431.
Minetti, A.E., Saibene, F., Ardigo, L.P., Atchou, G., Schena, F., Ferretti, G., 1994. Pygmy locomotion. Eur. J. Appl. Physiol. 68, 285–290.
Morton, D.J., 1922. The evolution of the human foot I. Am. J. Phys. Anthropol. 5, 305–336.
Myers, M., Steudel, K., 1985. Effect of limb mass distribution on the energetic cost of running. J. Exp. Biol. 16, 363–373.
Nagel, A., Fernholz, F., Kibele, C., Rosenbaum, D., 2008. Long distance running increases plantar pressures beneath the metatarsal heads-a barefoot walking investigation of 200 marathon runners. Gait Posture 27, 152–155.
O'Connell, J.F., Hawkes, K., Jones, N.G.B., 1999. Grandmothering and the evolution of *Homo erectus*. J. Hum. Evol. 36, 461–485.
Pontzer, H., 2005. A new model predicting locomotor cost from limb length via force production. J. Exp. Biol. 208, 1513–1524.
Pontzer, H., 2006. Locomotor Energetics, Ranging Ecology, and the Origin of the Genus *Homo*. Doctoral Dissertation, Harvard University.
Pontzer, H., 2007a. Limb length and the scaling of locomotor cost in terrestrial animals. J. Exp. Biol. 210, 1752–1761.
Pontzer, H., 2007b. Predicting the cost of locomotion in terrestrial animals: a test of the LiMb model in humans and quadrupeds. J. Exp. Biol. 210, 484–494.
Pontzer, H., Raichlen, D.A., Sockol, M.D., 2009. The metabolic cost of walking in humans, chimpanzees, and early hominins. J. Hum. Evol. 56, 43–54.
Reikeras, O., Bjerkreim, I., Kolbenstvedt, A., 1983. Anteversion of the acetabulum and femoral neck in normals and in patients with osteoarthritis of the hip. Acta Orthop. Scand. 54, 18–23.
Rightmire, G.P., Lordkipanidze, D., Vekua, A., 2006. Anatomical descriptions, comparative studies and evolutionary significance of the hominin skulls from Dmanisi, Republic of Georgia. J. Hum. Evol. 50, 115–141.
Rittmeister, M., Hanusek, S., Starker, M., 2006. Does tibial rotation correlate with femoral anteversion? Implications for hip arthroplasty. J. Arthroplasty 21, 553–558.
Rolian, C., Lieberman, D.E., Hamill, J., Scott, J.W., Werbel, W., 2009. Walking, running and the evolution of short toes in humans. J. Exp. Biol. 212, 713–721.
Ruff, C., 2007. Body size prediction from juvenile skeletal remains. Am. J. Phys. Anthropol. 133, 698–716.
Ruff, C.B., Trinkaus, E., Holliday, T.W., 1997. Body mass and encephalization in Pleistocene *Homo*. Nature 387, 173–176.
Ruff, C.B., Walker, A., 1993. Body size and body shape. In: Walker, A., Leakey, R.E. (Eds.), The Nariokotome *Homo erectus* Skeleton. Harvard University Press, Cambridge, pp. 234–265.
Shipman, P., Walker, A., 1989. The costs of becoming a predator. J. Hum. Evol. 18, 373–392.
Simpson, S.W., Quade, J., Levin, N.E., Butler, R., Dupont-Nivet, G., Melanie Everett, M., Semaw, S., 2008. A female *Homo erectus* pelvis from Gona, Ethiopia. Science 322, 1089–1092.
Singh, I., 1959. Squatting facets on the talus and tibia in Indians. J. Anat. 93, 540–550.
Steudel-Numbers, K., 2006. Energetics in *Homo erectus* and other early hominins: the consequences of increased lower limb length. J. Hum. Evol. 51, 445–453.
Steudel-Numbers, K.L., Tilkens, M.J., 2004. The effect of lower limb length on the energetic cost of locomotion: implications for fossil hominins. J. Hum. Evol. 47, 95–109.
Susman, R.L., de Ruiter, D.J., 2004. New hominin first metatarsal (SK 1813) from Swartkrans. J. Hum. Evol. 47, 171–181.
Susman, R.L., Stern, J.T., 1982. Functional morphology of *Homo habilis*. Science 217, 931–934.
Trinkaus, E., 1981. Neanderthal limb proportions and cold adaptation. In: Stringer, C. B. (Ed.), Aspects of Human Evolution. Taylor and Francis, London, pp. 187–219.
Vekua, A., Lordkipanidze, D., Rightmire, G.P., Agusti, J., Ferring, R., Maisuradze, G., Mouskhelishvili, A., Nioradze, M., Ponce de Leon, M., Tappen, M., Tvalchrelidze, M., Zollikofer, C., 2002. A new skull of early *Homo* from Dmanisi, Georgia. Science 297, 85–89.
Walker, A., 1993. Perspectives on the Nariokotome discovery. In: Walker, A., Leakey, R.E. (Eds.), The Nariokotome *Homo erectus* Skeleton. Harvard University Press, Cambridge, pp. 411–430.
Wallace, I.J., Demes, B., Jungers, W.L., Alvero, M., Sul, A., 2008. The bipedalism of the Dmanisi hominins: pigeon-toed early *Homo?* Am. J. Phys. Anthropol. 136, 375–378.
Ward, C.V., 2002. Interpreting the posture and locomotion of *Australopithecus afarensis*, where do we stand? Yearbk. Phys. Anthropol. 45, 185–215.
Webb, D., 1996. Maximum walking speed and lower limb length in hominids. Yearbk. Phys. Anthropol. 101, 515–525.
Wrangham, R.W., Jones, J.H., Laden, G., Pilbeam, D., Conklin-Brittain, N., 1999. The raw and the stolen: cooking and the ecology of human origins. Curr. Anthropol. 40, 567–594.
Young, N.M., Hallgrimsson, B., 2005. Serial homology and the evolution of mammalian limb covariation structure. Evolution 59, 2691–2704.
Yushiok, Y., Siu, D., Cooke, D.V., 1987. The anatomy and functional axes of the femur. J. Bone Joint Surg. 69, 873–880.

Please cite this article in press as: Pontzer, H., et al., Locomotor anatomy and biomechanics of the Dmanisi hominins, J Hum Evol (2010), doi:10.1016/j.jhevol.2010.03.006